This is a preprint, the final version is subject to change, of the American Mineralogist (MSA)
Cite as Authors (Year) Title. American Mineralogist, in press.
DOI: https://doi.org/10.2138/am-2019-6729

Revision #1

The Effect of Coordination Changes on the Bulk Moduli of Amorphous Silicates: The SiO_2-TiO_2 System as a Test Case

Quentin Williams[1], Murli H. Manghnani[2], Teruyuki Matsui[3]

[1]Dept. of Earth and Planetary Sciences, University of California, Santa Cruz, California, 95064 USA

[2]Hawaii Institute of Geophysics & Planetology, University of Hawaii, Honolulu, HI 96822 USA

[3]Knowledge Outsourcing Co., Inc, Nagoya, Japan

Abstract

The elasticity of a sequence of SiO_2-TiO_2 glasses is examined at high pressures and temperatures. A primary goal is to determine how the previously proposed substitution of 5-fold coordinate Ti at low concentrations of Ti and 4-fold coordinate Ti at higher concentrations affects the elastic properties of these glasses. The effect of changing Ti content on the bulk moduli of these glasses is monotonic, and no systematic effect of possible coordination changes is observed. In contrast, there is an apparent decrease in the pressure derivative of the bulk modulus above ~3 wt% TiO_2. This change occurs at a similar composition to that at which a transition from predominantly 5-fold to 4-fold of Ti has been proposed to occur in these glasses. Hence, this shift in the pressure derivative of the bulk modulus is attributed to a stiffening of the equation of state of these glasses generated by the substitution of 5-fold Ti species relative to TiO_4 units. Our results provide rationales for the onset of coordination changes producing a minimal change in the equation of state of silicate

melts/glasses, and for bulk moduli determined at ambient pressure producing relatively accurate silicate melt volumes even within liquids that have begun to undergo coordination changes. Thus, our results support the general validity of single equation of state formulations that describe the densities of silicate melts through the transition zone and shallow upper mantle.

Introduction

The densities of silicate melts at high pressures are of pivotal importance for a range of geophysical issues involving the differentiation and chemical evolution of the Earth. Densities of silicate melts at high pressures govern whether melts rise or sink at depth, with associated upward or downward transport of incompatible elements. And, the relationship between the pressure-dependence of the densities of melts and the shape of the melting curves of materials plays, via the Clausius-Clapeyron equation, a pivotal role in determining how magma oceans solidify (e.g., Andrault et al., 2011; Boukare et al., 2015). The densification of silicate melts at depth within Earth's transition zone and shallow upper mantle has long been recognized to hinge on coordination changes within network-forming components such as Si and Al, from 4-fold to higher coordinations (e.g., Waff, 1975; Williams and Jeanloz, 1988; Yarger et al., 1995; Farber and Williams, 1996; Stixrude and Karki, 2005). Despite these now well-documented coordination changes under pressure, the elastic properties of melts measured at ambient or low pressures (in a pressure range where few highly coordinated Si and Al atoms are anticipated to be present (e.g., Xue et al., 1991; Allwardt et al., 2005) are in fairly good accord with the

46 densities of liquids at conditions under which coordination changes almost certainly
47 have begun to occur within liquids. Specifically, the compaction of silicate liquids
48 under either static or shock loading into pressure ranges of 10's of GPa (e.g., Rigden
49 et al., 1989; Miller et al., 1993; Asimow and Ahrens, 2010; Thomas et al., 2012;
50 Sanloup et al., 2013)—a range that is associated with coordination changes
51 (typically, from four- to five- or six-fold) of network-forming cations within the
52 liquid structure--is, perhaps counter-intuitively, reasonably well predicted from
53 ambient pressure ultrasonic data on silicate liquids, which show that silicate liquids
54 have typical ambient pressure bulk moduli of 17-23 GPa (e.g., Manghnani et al.,
55 1986; Rivers and Carmichael, 1987; Secco et al., 1991; Ai and Lange, 2008). This
56 similarity raises the fundamental question: what is the effect of highly coordinated
57 species on the elasticity of silicate liquids in particular, and amorphous silicates in
58 general?

59 A straightforward means of evaluating the precise effect of coordination
60 changes on the elastic behavior of amorphous silicates involves making accurate
61 elastic measurements on a simple system in which a shift in coordination is well
62 documented. Previous measurements of elasticity of glasses under pressure (e.g.,
63 Sanchez-Valle and Bass, 2010; Liu and Lin, 2014) have not readily constrained the
64 precise interplay between complex, ill-constrained shifts in coordination (e.g., Fukui
65 and Hiroaka, 2018) and elasticity. In contrast to the multiple coordination
66 environments likely to be generated under compression, relatively well-
67 characterized changes in coordination induced by compositional changes at ambient
68 pressures can illuminate the degree to which a direct connection exists between

structural and elastic changes. In particular, titanium substitution in silica provides a test case with which to understand this issue of primary geophysical relevance: XANES spectroscopy by Henderson et al. (2002) has shown that glasses with up to ~3.6 wt% TiO_2 on the SiO_2-TiO_2 join have titanium present predominantly in 5-fold coordination, but four-fold Ti substitutes into these glasses at higher Ti concentrations, although a small fraction of 5-fold Ti is reported to persist. Similarly, Greegor et al. (1983) proposed, based on XANES and EXAFS that substitution of Ti into SiO_2 glass initially enters into the glass entirely in 6-fold coordination, but that the onset of 4-fold coordination occurs below 1 wt% TiO_2; Dingwell et al. (1994) reinterpreted their observations as indicating higher coordination (probably 5-fold) of Ti up to ~2 wt% TiO_2, with 4-fold at higher concentrations. A theoretical XANES study has suggested that the XANES peak assignments may differ from those utilized by experimentalists (Tamura et al., 2012), but there are extensive studies of the XANES of crystalline equivalents with known coordinations that validate the experimental assignments (e.g., Greegor et al., 1983; Dingwell et al., 1994; Farges, 1997; Henderson et al., 2002). That TiO_2 at low concentrations enters into silica in high coordination is also compatible with the behavior of Ti in a broad suite of silicate glasses (Farges, 1997). Thus, our study is oriented towards determining whether there is any variation in elastic properties of these glasses associated with the shift of Ti-substitution from high coordination at low concentrations (2-3.6 wt% TiO_2) to predominantly tetrahedral substitution at higher concentrations.

Five-fold coordination is predominantly associated, for typical magmatic compositions, with the coordination of aluminum under higher pressure conditions

(e.g., Allwardt et al., 2005), although there is substantial observational and theoretical evidence that five-fold silicon is of importance in magmatic compositions at deep upper mantle and transition zone conditions (e.g., Xue et al., 1991; Stixrude and Karki, 2005; Spera et al., 2011). Notably, glasses quenched to ambient conditions from high pressure melts in the 10 GPa range typically contain less than 10% of five-fold or six-fold Si (Xue et al., 1991; Allwardt et al., 2004). Similarly, the abundance of five-fold Si calculated to be present in $MgSiO_3$ liquid at transition zone conditions peaks at 30-50% abundance, with lower concentrations of six-fold silicon in this pressure range (Stixrude and Karki, 2005; Spera et al., 2011). Thus, the shift in coordination associated with several percent of Ti substitution within the SiO_2-TiO_2 system can provide a test for how higher coordinated titanium ions affectthe elastic properties relative to tetrahedrally-coordinated Ti.

In this instance, we are deploying chemical variations, and their associated shifts in coordination, as a proxy for the elastic effects of well-known pressure-induced changes in coordination in amorphous materials (e.g., Williams and Jeanloz, 1988; Xue et al., 1991; Farber and Williams, 1996; Shim and Catalli, 2009; Murakami and Bass, 2010; 2012). In particular, this system allows us to examine how the (presumably) weaker Si-O-$Ti^{V\text{-}fold}$ linkages and more highly coordinated Ti ions might impact the elasticity of glasses relative to Si-O-$(Si,Ti)^{IV\text{-}fold}$ linkages. While the system we examine is highly polymerized (i.e., the non-bridging oxygens/number of tetrahedral cations [NBO/T] ratio is nominally zero), it is notable that the NBO/T of mid-ocean ridge basalt is ~0.8 (e.g., Bauchy et al., 2013), and the degree of

114 polymerization of initial network cations will increase as their coordination number
115 increases.

116 The elastic properties of glasses and melts on the SiO_2-TiO_2 binary are also of
117 interest for a variety of petrologic, geophysical, and materials science reasons. First,
118 end-member SiO_2 is the prototypical polymerized silicate, and its properties have
119 been utilized to derive insights into the properties of crustal granitic and rhyolitic
120 melts (e.g., Ghiorso, 2004). Second, how titanium, one of the few major elements
121 (along with aluminum) that appears to substitute readily into silicate networks,
122 alters the properties of silicate melts has been a topic of ongoing interest for the
123 petrologic community (e.g., Farges et al., 1996; Liu and Lange, 2001). Third, the
124 anomalous thermal and elastic properties of end-member silica (a negative thermal
125 expansion and a negative pressure dependence of its bulk modulus) may extend to
126 geologically relevant melts, and particularly those of granitic chemistry (Hushur et
127 al., 2013). Lastly, the negative (and near-zero) thermal expansion of SiO_2-TiO_2
128 glasses, coupled with desirable optical properties, has generated their usage in a
129 range of applications in which low thermal expansions are needed, including optical
130 coatings, waveguides and mirror substrates (e.g., Andreatch and McSkimin, 1976;
131 Karasinski et al., 2015; Efthimiopoulos et al., 2018). Indeed, it is these thermal
132 properties and associated materials applications that have resulted in the extensive
133 structural characterizations of glasses in this compositional system.

134 Here, we present an integrated study of the elasticity of a sequence of TiO_2-
135 SiO_2 glasses at both ambient temperatures and high pressures, and high
136 temperatures at ambient pressure using ultrasonics, in order to probe the interplay

between the structure and elastic effects of titanium substitution into these silica-rich amorphous materials. Our results at high temperature are complementary to (but higher accuracy than) recent high-temperature studies using higher frequency Brillouin spectroscopy on (mostly) sol-gel synthesized glasses in this compositional system (Scannell et al., 2016), and cube resonance measurements made from 10-300 K (Hirao et al., 1995). The elasticity of a single composition in the TiO_2-SiO_2 system (with 7.4 wt% TiO_2) was measured by Andreatch and McSkimin (1974), but to pressures of only 0.12 GPa: we remeasure an aliquot of similar composition (ULE 7971A) in this study to substantially higher pressures.

Experimental Methods

The eight TiO_2-SiO_2 glasses used in this study were prepared by the flame hydrolysis boule process at the Corning Glass Works laboratory. The TiO_2 content of the glasses ranges from 1.3 to 9.4 wt % (Table 1). An end-member fused silica sample (Corning Code 7940) was also obtained from the Corning Glass Works. Samples from the boules from which our starting materials were cut have been compositionally characterized by X-ray fluorescence, with the accuracy of the compositions being estimated as ±0.1 wt% (Schultz and Smyth, 1972). Flame hydrolysis-synthesized glasses are deployed throughout this study: sol-gel glasses, which are equilibrated at lower temperatures, have notably lower elastic moduli (by 1.1-2.4 GPa) relative to higher temperature flame-synthesized glasses (Scannell et al., 2016). The glasses are optically clear, implying that no phase separation

occurred: such phase separation occurs at compositions containing >16.5 wt% TiO_2, and is characterized by the samples becoming translucent (e.g., Schultz, 1976).

The densities of the glass specimens were measured by the Archimedes method, using distilled water. The density and velocity measurements were made on the glasses both in an unannealed state, as well as after annealing: the annealed results are presented here. The annealing process involved heating the glasses to 1020˚C for about 1-1/2 hours, and then cooling them slowly from 1020 to 700˚C at a rate of 5˚C/hour, and then allowing them to cool inside the furnace from 700˚C to room temperature. This process ensures that the glass has no detectable hydroxyl contamination, which has been shown to strongly impact the sound velocities (Scannell et al., 2016), and removes internal strains from the glasses.

The ultrasonic velocities were measured by the pulse super-position method (a description of the apparatus utilized is given in Manghnani, 1972). Samples with an acoustic path length of about 1 cm were employed. The two faces of the sample were lapped flat within about 1 μm and parallel to within about 30 seconds of arc. X- and Y-cut 20 MHz quartz transducers, 0.63 cm in diameter, were used for compressional and shear wave velocity measurements, respectively. The sample was pressurized with a two stage nitrogen gas pressure-intensifying system. Pulse repetition frequencies were typically 200-500 KHz. The precision of the frequency f measurements is ~ 1 part in 10^5. The phase angle correction, $(\gamma/360)\,f$, produced by the bond between the transducer and the specimen, is negligible (γ does not exceed 2 degrees for a well prepared bond) and was ignored. For the high pressure measurements, the sample densities were corrected using the ambient pressure

bulk moduli for each composition determined in this study: this accurately simulates the density change over this limited pressure range. Densities in the high-temperature experiments were corrected using the thermal expansions determined by Schultz and Smyth (1972) for glasses in this compositional system. The resultant error in the velocity values reported here is considered to be less than 0.1%.

Results and Discussion

Figure 1 shows representative data taken under pressure on these glasses, with results given for each glass in Table 1. Although the pressure range is comparatively small, the accuracy of the data is high. The agreement of the pressure dependences with the previous ultrasonic work (at a frequency of 40 MHz) to 0.14 GPa of Andreatch and McSkimin (1976) on a ~7.5 wt% TiO_2 glass are excellent (Fig. 1); our absolute values of velocity for a glass of similar composition are 47 m/sec faster for compressional wave velocity and 28 m/sec for shear velocity (each are ~0.8% different). Yet, the sample density reported by Andreatch and McSkimin (1976) is slightly greater than that of our sample (by ~0.6%), so the impedance of the sample in the two studies is nearly identical.

As with silica glass and some haplogranitic compositions (e.g., Zha et al., 1994; Hushur et al., 2013 Manghnani), the observed velocities decrease with increasing pressure (Figure 1). This pressure-induced softening is generally viewed as a consequence of the potential surface associated with the Si-O-Si bond angle, the compaction of which is the primary means of low pressure compression (Huang and Kieffer, 2004; Liang et al., 2007). The trends in moduli with composition as titania

are shown in Figure 2; titania weakly decreases the density of the glasses (Table 1), but its effect on decreasing the compressibility of the glasses is substantially larger, in accord with ultrasonic experiments on titanium-bearing alkali silicate melts (Liu et al., 2007). This elastic softening is, to first-order, an entirely anticipated consequence of introducing weaker Ti-O bonds (Henderson et al., 2002) and hence broadened intertetrahedral angles into the structure through the incorporation of Ti (Chandrasekhar et al., 1979; Scannell et al., 2016). However, despite Ti adopting 5-fold coordination in the first few percent of substitution followed by 4-fold coordination at higher concentrations (e.g., Dingwell et al., 1994; Henderson et al., 2002; 2003), the trend of elasticity with composition is entirely monotonic. Within the resolution of our data, no difference in trend can be resolved between glasses at low Ti content and those at higher Ti content.

A notable aspect of the SiO_2-TiO_2 system, beyond the extensive amount of structural characterizations that have been conducted on glasses in this system, is that the substitution mechanism for titanium into the polymerized silicate matrix is fairly well-understood (e.g., Greegor et al., 1983; Dingwell et al., 1994; Henderson et al., 2002; 2003). Unlike in alkali- or alkali-aluminous Ti-bearing glasses in which there are interplays between the ratio of non-bridging oxygens to tetrahedral units (NBO/T), and network-modifying cation environment and the local bonding environment/coordination of titanium (e.g., Reynard and Webb, 1998; Liu et al., 2007), the substitution of Ti into a fully polymerized glass (NBO/T of 0) has straightforward structural consequences. Here, the substitution mechanism for

highly coordinated Ti (at low concentrations) involves the introduction of a five-fold coordinate Ti, which is anticipated to have weakened Si-O-Ti linkages.

Figure 2 shows the change in bulk and shear moduli as a function of composition. The bulk moduli from Ti-bearing flame-synthesized glasses determined by GHz Brillouin spectroscopy (Scannell et al., 2016) are greater than those determined in our MHz study, while the shear moduli are similar. The reasons for these differences are unclear, but differences in sample annealing history and/or the frequency of the probes may each play a role.

From a first-order elastic standpoint (Figure 2), the substitution of a five-fold Ti at low Ti-contents appears to have an indistinguishable effect to adding a more weakly bonded tetrahedral cation: or, phrased another way, the substitution of a highly coordinated cation is effectively elastically silent relative to the same cation substituting into a network site. This silence plausibly arises from the elastic effect of the highly coordinated cation (which is likely more rigid than the Si-O-Si network) being counter-balanced by the weakened, and thus more flexible, Si-O-$Ti^{V\text{-}fold}$ angles.

Unlike the bulk modulus, the pressure derivative of the bulk modulus (dK/dP) may show a small, but measureable, signature of the structural change associated with shifts in coordination of Ti (Figure 3). Here, although substituting Ti into these glasses is anticipated to make them more compressible and lower their dK/dP, the values of this parameter for low Ti glasses are nearly constant and near -5.5. Samples more enriched in Ti (with dominantly four-fold coordination) have K' values that average near -5.9 (Figure 3), in accord with the expectation that such

glasses are more compressible under pressure. The notable aspect here is that a change in speciation associated with a small quantity of Ti may produce an effect that is resolvable on *K'*: if this effect scales with the abundance of highly coordinated cations, then the K' values of amorphous materials undergoing high-pressure coordination changes could be markedly shifted. For comparison, the pressure derivatives of the shear moduli are notably constant throughout this range: this plausibly reflects that the shear modulus of these glasses is governed by the rigidity of the tetrahedral network, which is likely minimally altered by Ti substitution. For comparison, the bulk modulus reflects an averaged response of all of the structural components within the glass, and particularly its weakest bonded (and Ti-associated) components. Nevertheless, the key result here is that the pressure derivative of the bulk modulus may vary in a manner that reflects the coordination changes occurring within the glass, while the bulk modulus varies (within resolution) in a constant manner irrespective of Ti coordination. It is probable that titanium-bearing systems can provide other tests of this result. For example, glasses in the Na_2O-TiO_2-SiO_2 system vary substantially in their ratio of five-fold to six-fold titanium (Ponader et al., 1996), and such glasses have marked variations in their pressure derivatives of bulk moduli (Manghnani, 1972). However, distinguishing the elastic effects of shifting chemistry in ternary systems from those associated with changes in coordination will require more extensive elastic (and probably structural) data on different glass compositions than currently exists.

The observation of little variation in bulk modulus associated with a possible structural change is in accord with the general observation that shock data on silicate liquids to transition zone and upper lower mantle conditions can be fit with ambient pressure ultrasonic values of the bulk moduli, with values of dK/dP being variable fit parameters (e.g., Miller et al., 1991; Asimow and Ahrens, 2010), and emphasizes that dK/dP is likely the pivotal determining factor in modeling the equations of state of silicate liquids through coordination changes.

Pressure Dependence of Thermal Expansion

In order to draw constraints on the pressure dependence of the thermal expansion (α) of these glasses ($d\alpha/dP$, which is equivalent to $1/K^2(dK/dT)$), we also measured the temperature dependence of the sound velocities (Figure 4). In general, the temperature dependences of our results are slightly lower than those of the two fusion-synthesized SiO_2-TiO_2 glasses measured at high temperatures using Brillouin spectroscopy by Scannell et al. (2016).Modest elevations of longitudinal velocities (but not shear, as is indicated in Figure 2) in Brillouin measurements relative to ultrasonic measurements have been observed in silica glass (Vacher et al., 1981) due to relaxational effects, and we speculate that such effects are enhanced by temperature and could be responsible for the differences in temperature dependence between the results of Scannell et al. (2016) and our own (Fig. 5).

As with the negative shifts of velocity under pressure, the temperature-dependent velocities shift positively with increasing temperature. The corresponding bulk moduli also markedly stiffen (Fig. 5). Here, it is apparent that the values of the temperature derivatives of the moduli decrease with increases in

295 TiO_2 content. That is, the glasses become less anomalous in their thermal behavior
296 as titanium content increases, in contrast to the more anomalous behavior of glasses
297 richer in Ti under pressure. The detailed effects of annealing and temperature and
298 pressure on the Lamé parameters of glasses in this system will be discussed in a
299 later contribution.

300 The contributions to total change in the bulk modulus, K, due to temperature
301 effects can be considered in terms of intrinsic and extrinsic parts:

302 $$dK = (\partial K/\partial T)_V \, dT + (\partial K/\partial V)_T \, dV \qquad (1)$$

303 Here, the first term on the right of Eqn. 1 involves intrinsic, temperature-induced,
304 changes to the bulk modulus, while the second term involves extrinsic changes
305 induced by volumetric shifts. Eqn. 1 can be rearranged as:

306 $$(dK/dT)_P = (\partial K/\partial T)_V - \alpha K \, (\partial K/\partial P)_T \qquad (2)$$

307 Using the data in Tables 1 and 2, and thermal expansion coefficients from
308 Schultz and Smyth (1972), the intrinsic and extrinsic contributions to the
309 temperature-dependence of the moduli can be calculated. For all compositions, the
310 intrinsic portion is over 99% of the net temperature shift of the bulk modulus: this
311 dominance is largely a consequence of the low thermal expansion of these glasses.
312 Hence, the temperature-dependent moduli depend almost entirely on thermal, not
313 volumetric effects. Thus, there is a straightforward rationale for the differing
314 behavior of the trend of the temperature dependence of the moduli with
315 composition (becoming less anomalous) from the pressure dependence of the
316 moduli with composition (which become more anomalous, with more negative

317 dK/dP's), in that the former hinges on thermal effects, while the latter hinges on
318 volumetric effects.

319 Figure 6 shows estimated values of the change in thermal expansion with
320 pressure as a function of composition. There may be an indication that the low-Ti
321 compositional domain that is associated with 5-fold Ti coordination may have a
322 somewhat different trend than the rest of the glasses, but this effect is not well-
323 resolved. A novel aspect of Figure 6 is that it predicts that SiO_2-TiO_2 glasses should,
324 at modest pressures, have notably positive thermal expansions: that is, the near-
325 zero thermal expansions associated with these glasses at ambient pressure is a
326 fragile phenomenon that is removed by compaction.

327

328 **Geophysical Implications**

329 A long-standing question in the study of magmatic silicates under pressure
330 is: How does one extrapolate the volume of a silicate liquid into a regime in which
331 coordination changes become important for different network components? Like
332 solids, does this structural change involve a discontinuity (smeared-out within the
333 liquid) in volume and elastic properties? Or is the coordination transition not
334 readily elastically detectable?

335 Our highly accurate low-pressure and high-temperature elastic results, on a
336 system known to undergo a coordination change at ambient conditions, distinctly
337 favor the coordination transition not being easily elastically detectable. The
338 rationale for this outcome appears to be that, unlike in crystalline equivalents,
339 introducing a highly coordinated cation into an amorphous material produces

additional structural changes, which includes the creation of weaker polyhedral linkages. Thus, the net total elastic effects of the genesis of a highly coordinated cation comprise a set of complex structural/bonding changes that, at least within the TiO_2-SiO_2 system, appear to have little resolvable effect on the bulk modulus of the material; however, an effect on the pressure derivative of the bulk modulus may be generated.

The consequences of this observation are multi-fold. First, simulations of silicate melts that incorporate a single equation of state are likely to be able to accurately simulate the high pressure volumes and elasticity of silicate liquids as coordination changes commence. Second, given an ambient pressure bulk modulus, the pressure derivative of the bulk modulus may prove to be a key parameter in assessing the density and elasticity of silicate melts within the transition zone and shallow lower mantle. Third, because of the possible variation in the pressure derivative of the bulk modulus that we observe as a function of cation coordination, such derivatives should optimally be constrained *in situ* at pressure.

Acknowledgments.

We deeply appreciate the help of the late John Balogh in maintaining the facilities and conducting these experiments. We are very thankful to Dr. Peter C. Schultz and the Corning Glass Works for supplying the glass samples for this project, and two reviewers for helpful comments. This work was supported by NSF grant 0757137 (to MHM) and NSF-EAR1620423 (to QW).

363

364 **References**

365 Ai, Y., and Lange R.A. (2008) New acoustic velocity measurements on CaO-MgO-
366 Al_2O_3-SiO_2 liquids: Reevaluation of the volume and compressibility of $CaMgSi_2O_6$-
367 $CaAl_2Si_2O_8$ liquids to 25 GPa, *Journal of Geophysical Research, 113,* B04203.
368 Allwardt, J.R., Schmidt, B.C., Stebbins, J.F. (2004) Structural mechanisms of
369 compression and decompression in high-pressure $K_2Si_4O_9$ glasses: An investigation
370 utilizing Raman and NMR spectroscopy of glasses and crystalline materials,
371 Chemical Geology, 213, 137-151.
372 Allwardt, J.R., Stebbins, J.F., Schmidt, B.C., Frost, D.J., Withers, A.C. and Hirschmann,
373 M.M. (2005) Aluminum coordination and the densification of high-pressure
374 aluminosilicate glasses, *American Mineralogist, 90,* 1218-1222.
375 Andrault, D., et al. (2011) Solidus and liquidus profiles of chondritic mantle:
376 Implication for melting of the Earth across its history, *Earth and Planetary Science*
377 *Letters, 304,* 251-259.
378 Andreatch, P. and McSkimin, H.J. (1976) Pressure dependence of ultrasonic wave
379 velocities and elastic stiffness moduli for a TiO_2-SiO_2 glass (Corning 7971), *Journal of*
380 *Applied Physics, 47,* 1299-1301.
381 Asimow, P., and Ahrens, T.J. (2010) Shock compression of liquid silicates to 125 GPa:
382 The anorthite-diopside join, *Journal of Geophysical Research, 115,* B10209.
383 Bauchy, M., Guillot, B., Micoulaut, M., and Sator, N. (2013) Viscosity and viscosity
384 anomalies of model silicates and magmas: A numerical investigation, *Chemical*
385 *Geology, 346,* 47-56.

386 Boukare, C.E., Ricard, Y. and Fiquet, G. (2015) Thermodynamics of the MgO-FeO-SiO_2
387 system up to 140 GPa: Application to the crystallization of Earth's magma ocean,
388 *Journal of Geophysical Research, 120,* 6085-6101.
389 Chandrasekhar, H.R., Chandrasekhar, M. and Manghnani, M.H. (1979) Phonons in
390 titanium-doped vitreous silica, *Solid State Communications, 31,* 329-333.
391 Dingwell, D.B., Paris, E., Seifert, F., Mottana, A., and Romano, C. (1994) X-ray
392 absorption study of Ti-bearing silicate glass, *Physics and Chemistry of Minerals, 21,*
393 501-509.
394 Efthimiopoulos, I., et al., Femtosecond laser-induced transformations in ultra-low
395 expansion glass: Microstructure and local density variations by vibrational
396 spectroscopy, *Journal of Applied Physics, 123,* 233105, 2018.
397 Farber, D.L., and Williams, Q. (1996) An in situ Raman spectroscopic study of
398 $Na_2Si_2O_5$ at high pressures and temperatures: Structures of compressed liquids and
399 glasses, *American Mineralogist, 81,* 273-283.
400 Farges, F. (1997) Coordination of Ti^{4+} in silicate glasses: A high resolution XANES
401 spectroscopy study at the Ti K-edge. *American Mineralogist, 82,* 36-43.
402 Farges, F., Brown, G.E., Navrotsky, A., Gan, H. and Rehr, J.J. (1996) Coordination
403 chemistry of Ti(IV) in silicate glasses and melts: II. Glasses at ambient temperature
404 and pressure. *Geochimica et Cosmochimica Acta, 60,* 3039-3053.
405 Fukui, H., and Hiraoka N. (2018) Electronic and local atomistic structure of $MgSiO_3$
406 glass under pressure: A study of X-ray Raman scattering at the silicon and
407 magnesium L-edges, *Physics and Chemistry of Minerals, 45,* 211-218.

Ghiorso, M.S. (2004) An equation of state for silicate melts: Formulation of a general model, *American Journal of Science, 304,* 637-678, 2004.

Gonzalez-Oliver, C.J.R., James, P.F. and Rawson, H. (1982) Silica and silica-titania glasses prepared by the sol-gel process, *Journal of Non-Crystalline Solids, 48,* 129-152.

Greegor, R.B., Lytle, F.W., Sandstrom, D.R., Wong, J., and Schultz, P. (1983) Investigation of TiO_2-SiO_2 glasses by X-ray absorption spectroscopy, *Journal of Non-Crystalline Solids, 55,* 27-43.

Henderson, G.S., Liu, X., and Fleet, M.E. (2002) A Ti L-edge X-ray absorption study of Ti-silicate glasses, *Physics and Chemistry of Minerals, 29,* 32-42.

Henderson, G.S., Liu, X., and Fleet, M.E. (2003) Titanium coordination in silicate glasses investigated using O K-edge X-ray absorption spectroscopy, *Mineralogical Magazine, 67,* 597-607.

Hirao, K., Tanaka, K., Furukawa, S. and Soga, N. (1995) Anomalous temperature dependence of the sound velocities of SiO_2-TiO_2 glasses, *Journal of Materials Science Letters, 14,* 697-699.

Huang, L. and Kieffer, J. (2004) Amorphous-amorphous transitions in silica glass. I. Reversible transitions and thermomechanical anomalies, *Physical Review B, 69,* 224203.

Hushur, A., Manghnani, M.H., Williams, Q. and Dingwell, D.B. (2013) A high-temperature Brillouin scattering study on four compositions of haplogranitic glasses and melts: High-frequency elastic behavior through the glass transition, *American Mineralogist, 98,* 367-375.

Karasinski, P., Tyszkiewicz, C., Maciaga, A., Kityk, I.V., and Gondek, E. (2015) Two-component waveguide SiO_2:TiO_2 films fabricated by sol-gel technology for optoelectronic applications, *Journal of Materials Science, 26,* 2733-2736.

Liang, Y. Miranda, C.R. and Scandolo, S. (2007) Mechanical strength and coordination defects in compressed silica glass: Molecular dynamics simulations, *Physical Review B, 75,* 024205.

Liu, Q. and Lange, R.A. (2001) The partial molar volume and thermal expansivity of TiO_2 in alkali silicate melts: Systematic variation with Ti coordination, *Geochimica et Cosmochimica Acta, 65,* 2379-2392.

Liu, Q., Lange, R.A., and Ai, Y. (2007) Acoustic velocity measurements on Na_2O-TiO_2-SiO_2 liquids: Evidence for a highly compressible TiO_2 component related to five-coordinated Ti, *Geochimica et Cosmochimica Acta, 71,* 4314-4326.

Liu, J. and Lin, J.-F. (2014) Abnormal acoustic wave velocities in basaltic and (Fe-Al)-bearing silicate glasses at high pressure, Geophysical Research Letters, 41, 8832-8839.

Manghnani, M.H. (1972) Pressure and temperature dependence of the elastic moduli of Na_2O-TiO_2-SiO_2 glasses, *Journal of the American Ceramic Society, 55,* 360-365.

Manghnani, M.H., Sato, H. and Rai, C.S. (1986) Ultrasonic velocity and attenuation measurements on basalt melts to 1500°C: Role of composition and structure in the viscoelastic properties, *Journal of Geophysical Research, 91,* 9333-9342.

452 Miller, G.H., Stolper, E.M., and Ahrens, T.J. (1991) The equation of state of molten
453 komatiite: 1. Shock wave compression to 36 GPa, *Journal of Geophysical Research, 96,*
454 11831-11848.
455 Murakami, M., and Bass, J.D. (2010) Spectroscopic evidence for ultrahigh-pressure
456 polymorphism in SiO_2 glass, *Physical Review Letters, 104,* 025504.
457 Murakami, M., and Bass, J.D. (2011) Evidence of denser $MgSiO_3$ glass above 133 GPa
458 and implications for remnants of ultradense melt from a deep magma ocean,
459 *Proceedings of the National Academy of Sciences, 108,* 17286-17289.
460 Ponader, C.W., Boek, H., Dickinson, J.E., Jr. (1996) X-ray absorption study of the
461 coordination of titanium in sodium-titanium-silicate glasses, *Journal of Non-*
462 *Crystalline Solids, 201,* 81-94.
463 Reynard, B., and Webb, S. (1998) High-temperature Raman spectroscopy of
464 $Na_2TiSi_2O_7$ glass and melt: Coordination of Ti^{4+} and nature of the configurational
465 changes in the liquid, *European Journal of Mineralogy, 10,* 49-58.
466 Rigden, S.M., Ahrens, T.J. and Stolper, E.M. (1989) High-pressure equation of state of
467 molten anorthite and diopside, *Journal of Geophysical Research, 94,* 9508-9522.
468 Rivers, M.L., and Carmichael, I.S.E. (1987) Ultrasonic studies of silicate melts, *Journal*
469 *of Geophysical Research, 92,* 9247-9270.
470 Sanchez-Valle, C., and Bass, J.D. (2010) Elasticity and pressure-induced structural
471 changes in vitreous $MgSiO_3$-enstatite to lower mantle pressures. *Earth and Planetary*
472 *Science Letters, 391*, 288-295.
473 Sanloup, C., et al. (2013) Structural change in molten basalt at deep mantle
474 conditions, *Nature, 503,* 104-107.

475 Scannell, G., Koike, A., and Huang, L. (2016) Structure and thermo-mechanical
476 response of TiO_2-SiO_2 glasses to temperature, *Journal of Non-Crystalline Solids, 447,*
477 238-247.
478 Schultz, P.C. (1976) Binary titania-silica glasses containing 10 to 20 wt% TiO_2,
479 *Journal of the American Ceramic Society, 59,* 214-219.
480 Schultz, P. and Smyth, G.T. (1972) Ultra-low expansion glasses and their structure in
481 the SiO_2-TiO_2 system, in *Amorphous Materials*, edited by R.W. Douglas and B. Ellis,
482 Wiley-Interscience, New York, 453-461.
483 Secco, R.A., Manghnani, M.H., and Liu, T.-C. (1991) Velocities and compressibililities
484 of komatiitic melts, *Geophysical Research Letters, 18,* 1397-1400.
485 Shim, S.-H., and Catalli, K. (2009) Compositional dependence of structural transition
486 pressures in amorphous phases with mantle-related compositions, *Earth and*
487 *Planetary Science Letters, 283,* 174-180.
488 Spera, F.J., Ghiorso, M.S., and D. Nevins (2011) Structure, thermodynamic and
489 transport properties of liquid $MgSiO_3$: Comparison of molecular models and
490 laboratory results, *Geochimica et Cosmochimica Acta, 75,* 1272-1296.
491 Stixrude, L., and Karki, B. (2005) Structure and freezing of $MgSiO_3$ liquid in Earth's
492 lower mantle, *Science, 310,* 297-299.
493 Tamura, T., Tanaka, S., and Kohyama, M. (2012) Full PAW calculations of
494 XANES/ELNES spectra of Ti-bearing oxide crystals and TiO-SiO glasses: Relation
495 between pre-edge peaks and Ti coordination, *Physical Review B, 85,* 205210

Thomas, C., Liu, Q., Agee, C.B., Asimow, P.D., and Lange, R.A. (2012) Multi-technique equation of state for Fe_2SiO_4 melt and the density of Fe-bearing silicate melts form 0 to 161 GPa, *Journal of Geophysical Research, 117,* B10206.

Vacher, R., Pelous, J., Plicque F., and Zermbowitch, A. (1981) Ultrasonic and Brillouin scattering study of the elastic properties of vitreous silica between 10 and 300 K. *Journal of Non-Crystalline Solids, 45,* 397-410.

Waff, H. (1975) Pressure-induced coordination changes in magmatic liquids, *Gephysics Research Letters, 2,* 193-196.

Williams, Q. and R. Jeanloz (1988) Spectroscopic evidence for pressure-induced coordination changes in silicate glasses and melts, *Science, 239,* 902-905.

Xue, X., Stebbins, J.F., Kanzaki, M., McMillan, P.F., and Poe, B. (1991) Pressure-induced silicon coordination and tetrahedral structural changes in alkali oxide-silica melts up to 12 GPa: NMR, Raman, and infrared spectroscopy, *American Mineralogist, 76,* 8-26.

Yarger, J.L., et al. (1995) Al coordination changes in high-pressure aluminosilicate liquids, *Science, 270,* 1964-1967.

Zha, C-S., Hemley, R.J., Mao, H.-K., Duffy, T.S. and Meade, C. (1994) Acoustic velocities and refractive index of SiO_2 glass to 57.5 GPa by Brillouin scattering, *Physical Review B, 50,* 13105-13112.

Figure Captions.

Figure 1. Representative data on compressional (P) and shear (S) wave velocities for two compositions of glass under pressure. The lines without symbols are results for

519 a ~7.5 wt% TiO_2 glass reported by Andreatch and McSkimin (1976). Typical errors
520 on velocities are 0.1%, or substantially smaller than the symbols.
521
522 Figure 2. Variations in bulk and shear moduli with composition at 300 K. The
523 horizontal bar denotes the compositional range in which predominantly 5-fold Ti-
524 substitution has been proposed to take place (e.g., Henderson et al., 2002); greater
525 Ti-contents are dominated by 4-fold coordination. Open symbols show Brillouin
526 results on glasses formed by flame hydrolysis from Scannell et al. (2016); their sol-
527 gel glasses lie at 1.1-2.4 GPa lower moduli than the corresponding flame hydrolysis
528 glasses for all overlapping compositions.
529
530 Figure 3. Dependence of the pressure derivatives of the bulk and shear moduli on
531 titania composition. Two possible fits to the dK/dP data are shown: the smooth
532 curve (red) is a simple quadratic fit that might reflect a gradual coordination shift,
533 while the latter (black) reflects possible non-linear behavior in the compositional
534 range in which Ti shifts coordination from 5-fold to 4-fold within these glasses. The
535 data do not discriminate between these fits.
536
537 Figure 4. Representative velocity measurements at high temperatures; the onset of
538 the high frequency glass transition causes the notable decline in velocities in excess
539 of 800°C for the 4.6% TiO_2 composition, and a combination of the glass transition
540 and possible unmixing of the glass (e.g., Gonzalez-Oliver et al., 1982) impact the 9.4
541 wt% sample at the highest temperature conditions.

Figure 5. Bulk moduli of SiO_2-TiO_2 glasses at high temperatures; the onset of the high frequency glass transition causes the notable decline in modulus in excess of 800°C for the 4.6% TiO_2 composition, and crystallization of TiO_2 from the 9.4 wt% sample causes the increase in modulus for this composition. The shaded lines (red online) show the bulk moduli trends from the Brillouin spectroscopy study of Scannell et al. (2016) for their glasses with 7.05 wt% (upper) and 10.7 wt% (lower) TiO_2 contents.

Figure 6. Estimated change in thermal expansion with pressure as a function of titania content, as derived from the bulk modulus and its temperature dependence. The correction term from isentropic to isothermal bulk modulus is negligibly small in these low thermal expansion glasses (Schultz and Smyth, 1970), and hence is ignored.

This is a preprint, the final version is subject to change, of the American Mineralogist (MSA)
Cite as Authors (Year) Title. American Mineralogist, in press.
DOI: https://doi.org/10.2138/am-2019-6729

557 **Tables.**

558 **Table 1. Chemical composition and elastic parameters of SiO_2-TiO_2 glasses at**
559 **ambient pressure and temperature.**
560
561
562
563
564
565

Glass Number	Composition in wt % SiO_2	TiO_2	ρ g/cm^3	V_P km/sec (±0.006)	V_S km/sec (±0.004)	K GPa (±0.09)	μ GPa (±0.06)
7940A (fused silica)	100	0	2.2007	5.947	3.769	36.16	31.26
T4A	98.7	1.3	2.2005	5.911	3.746	35.71	30.88
T1A	97.2	2.8	2.2001	5.872	3.717	35.32	30.40
T5A	95.4	4.6	2.1995	5.833	3.692	34.87	29.98
T6A	94.0	6.0	2.1992	5.803	3.672	34.53	29.65
T2A	92.7	7.3	2.1986	5.758	3.635	34.15	29.05
ULE 7971A	92.5	7.5	2.1993	5.783	3.653	34.42	29.35
T3A	90.6	9.4	2.1985	5.719	3.607	33.77	28.60

This is a preprint, the final version is subject to change, of the American Mineralogist (MSA)
Cite as Authors (Year) Title. American Mineralogist, in press.
DOI: https://doi.org/10.2138/am-2019-6729

Table 2. Pressure and temperature derivatives of the elastic parameters of SiO_2-TiO_2 glasses at ambient conditions.

Glass Number	dK/dP	dμ/dP	dK/dT GPa/deg	dμ/dT GPa/deg
7940A (silica)	-5.37	-3.53	.0124	.0051
T4A	-5.68	-3.56	.0121	.0052
T1A	-5.42	-3.56	.0121	.0050
T5A	-5.97	-3.55	.0119	.0050
T6A	-5.85	-3.54	.0119	.0048
T2A	-5.96	-3.60	.0120	.0048
ULE 7971A	-5.88	-3.60	.0119	.0047
T3A	-5.77	-3.59	.0117	.0047

This is a preprint, the final version is subject to change, of the American Mineralogist (MSA)
Cite as Authors (Year) Title. American Mineralogist, in press.
DOI: https://doi.org/10.2138/am-2019-6729

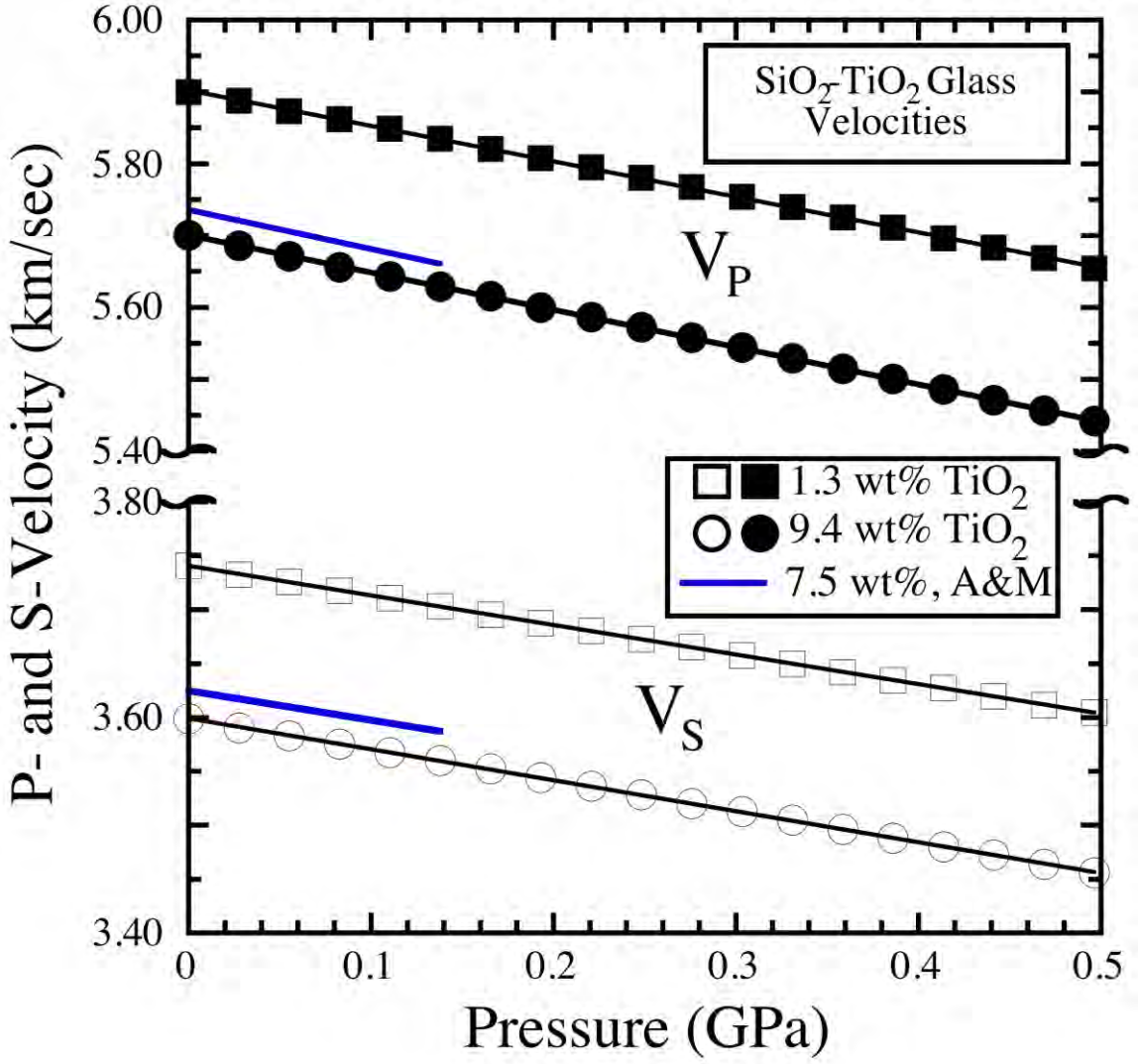

583
584 Figure 1.

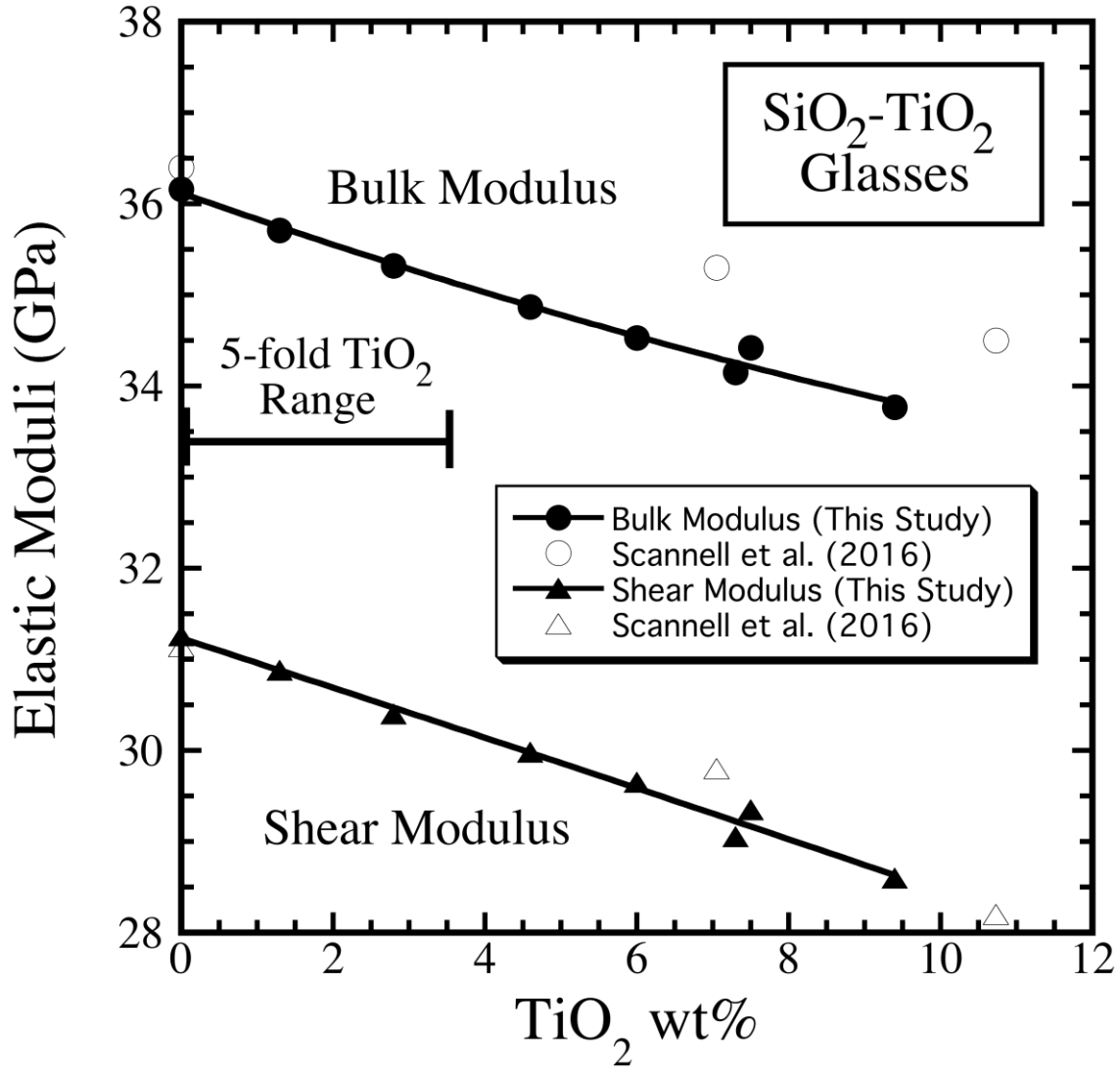

585

586 Figure 2.

587

588

This is a preprint, the final version is subject to change, of the American Mineralogist (MSA)
Cite as Authors (Year) Title. American Mineralogist, in press.
DOI: https://doi.org/10.2138/am-2019-6729

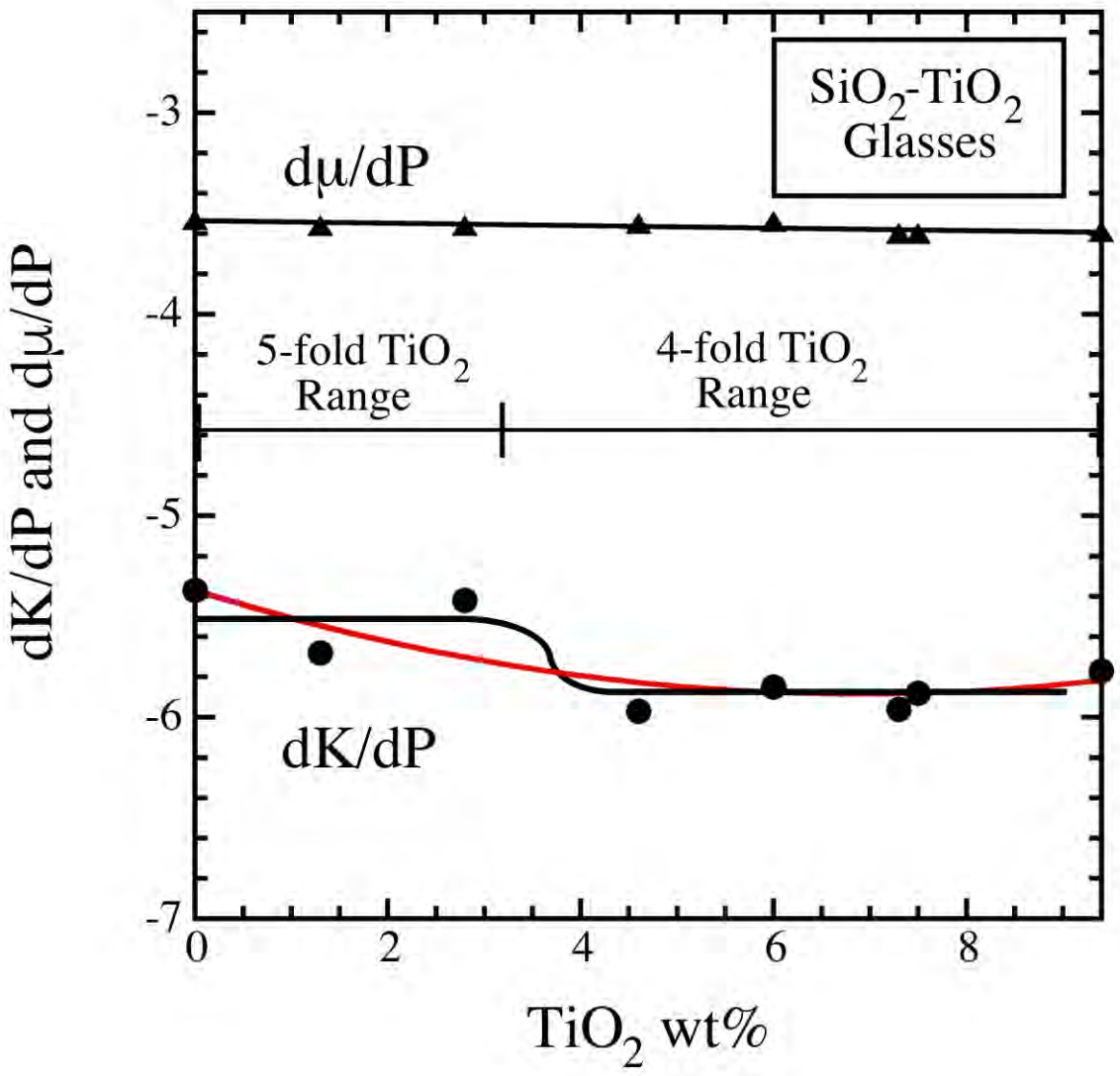

589

590

591 Figure 3.

This is a preprint, the final version is subject to change, of the American Mineralogist (MSA)
Cite as Authors (Year) Title. American Mineralogist, in press.
DOI: https://doi.org/10.2138/am-2019-6729

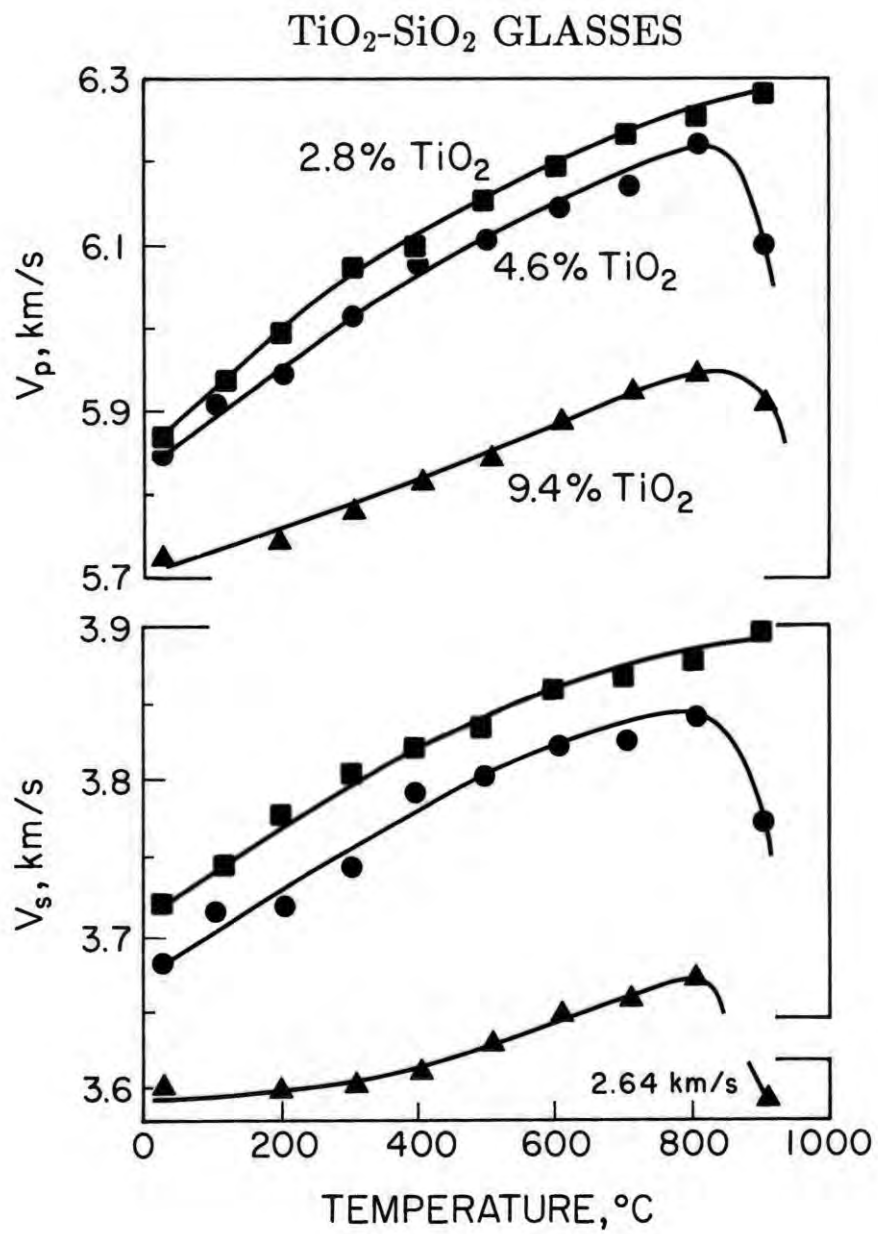

592

593 Figure 4.

594

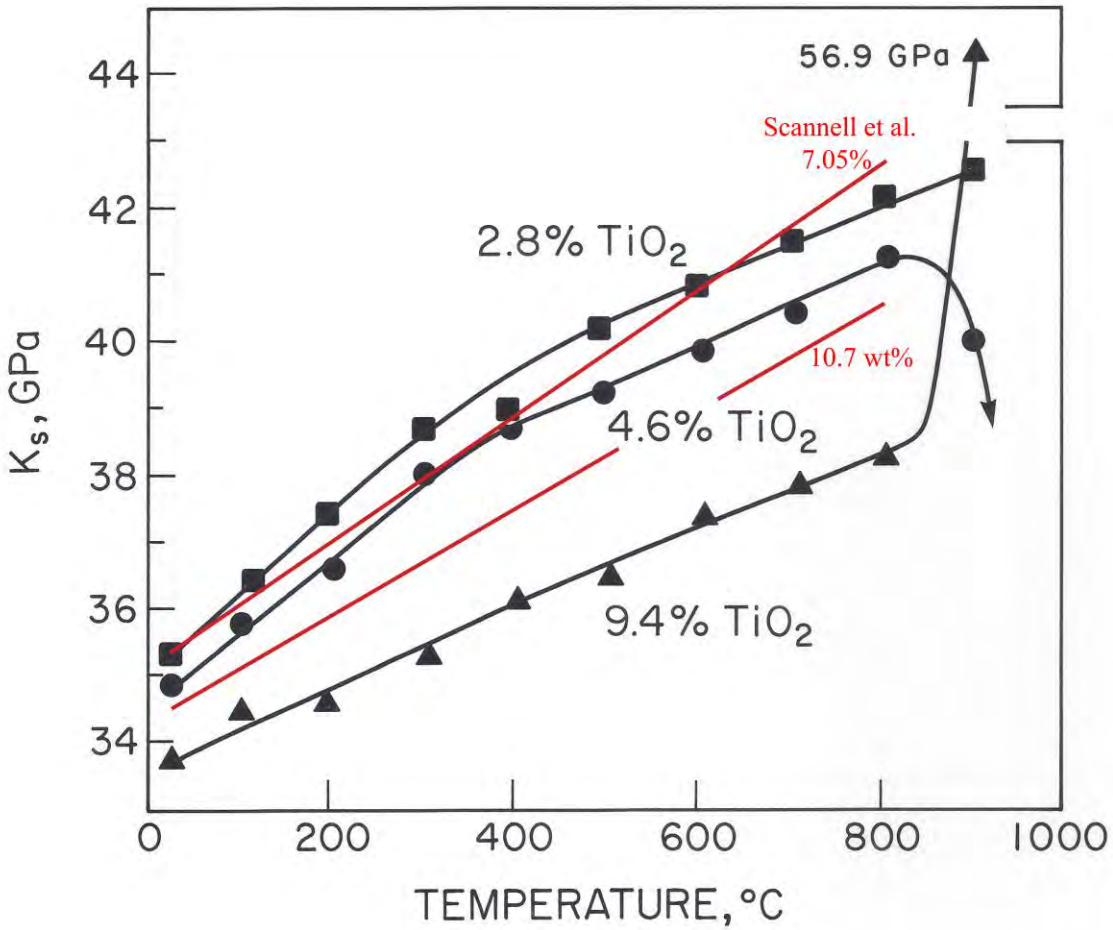

595

596 Figure 5.

597

This is a preprint, the final version is subject to change, of the American Mineralogist (MSA)
Cite as Authors (Year) Title. American Mineralogist, in press.
DOI: https://doi.org/10.2138/am-2019-6729

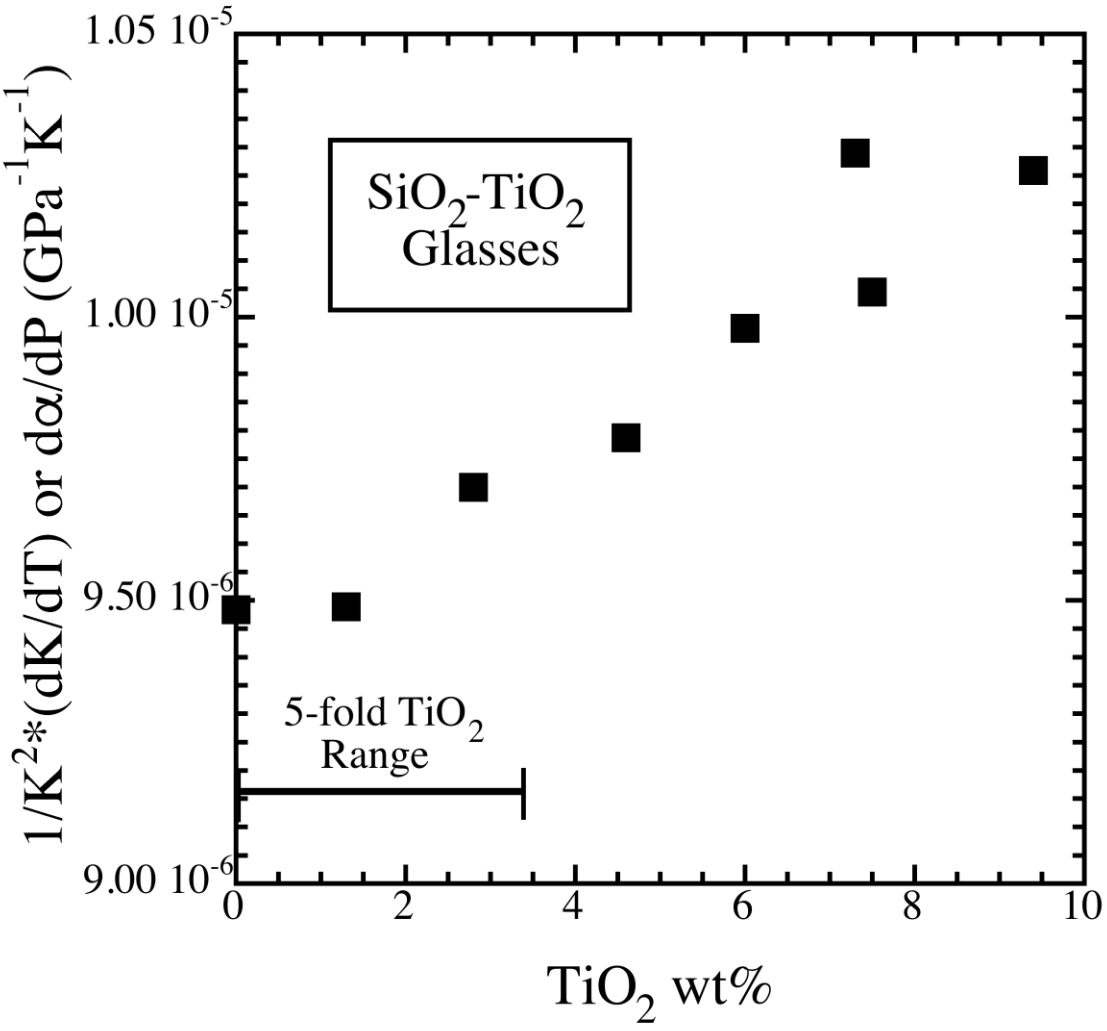

598

599 Figure 6.

600